Performance Scaling Laws for PD Array-based Receivers in IM/DD Optical Wireless Communication Systems

Aravindh Krishnamoorthy[©]*, *Member, IEEE,* Robert Schober[†], *Fellow, IEEE,* Harald Haas*, *Fellow, IEEE*

* LiFi Research and Development Centre, Electrical Engineering Division, University of Cambridge, UK,
† Institute for Digital Communications, Friedrich-Alexander-Universität Erlangen-Nürnberg, Germany

Abstract—**We study the performance scaling laws for electrical-domain combining in photodetector (PD) array-based receivers employing intensity modulation and direct detection, taking into account the inherent square-law relationship between the optical and electrical received powers. The performance of PD array-based systems is compared, in terms of signal-to-noise ratio (SNR) and achievable rate, to that of a reference receiver employing a single PD. Analytical and numerical results show that PD arrays provide performance gains for sufficiently narrow beams and above an SNR threshold. Furthermore, increasing the number of PDs alone does not enhance performance, and joint optimization of beam pattern, transverse electromagnetic mode, received power, and PD positions is necessary. Our model and derived insights provide practical guidelines and highlight the trade-offs for the design of next-generation high-bandwidth PD array receivers.**

I. INTRODUCTION

Laser-based intensity modulation and direct detection (IM/DD) optical wireless communication (OWC) systems find widespread use owing to their superior performance and low complexity. In these systems, at the transmitter, a laser's output intensity is modulated by an electrical signal, and at the receiver, the photocurrent from the received optical signal is directly converted to an electrical signal via a transimpedance amplifier (TIA). Hence, unlike coherent systems [1], no output phase control and local oscillators are needed at the transmitter and receiver, respectively, which lowers the system complexity significantly.

However, since quadrature modulation cannot be utilized in IM/DD systems, their spectral efficiency is half that of coherent optical systems [2], [3]. Furthermore, their sensitivity is low due to the lack of local oscillators. Nevertheless, with careful beam management and by exploiting the large, unlicensed bandwidth at optical frequencies, IM/DD links can exceed data rates of 1 Tbps [4], [5].

The capacity and achievable rates of IM/DD systems have been studied in detail [2], [3], [6]. Furthermore, technologies such as light fidelity (LiFi) [7] based on IM/DD systems have been proposed. More recently, in order to enhance performance, robustness to misalignment, and design and deployment flexibility, photodetector (PD) array-based receivers have been proposed [8]–[13].

In PD array-based receivers, instead of a single PD, an array of PDs is utilized. Furthermore, the electrical signals generated by the incident beam are optimally combined in the electrical domain. Moreover, since the active areas of the PDs are smaller compared to a single reference PD, their bandwidth can be enhanced via careful design [14]. However, in square-law detection systems, such as IM/DD systems, the received

electrical power is proportional to the square of the received optical power [14], [15]. Taking this into account is important for systems that combine signals in the electrical domain, see [16], [17]. However, a systematic study of the impact of the square-law relationship is not available in the literature.

Therefore, in this letter, we study the performance scaling laws for electrical-domain combining in PD arrays, taking into account the above square-law relationship. In particular, we compare their performance to a single reference PD for Gaussian, Laguerre-Gaussian (LG), and uniform laser beam patterns, which realize different levels of beam concentration on the PD array. We consider two different design choices: (1) The combined active area of the PD array scales with the number of PDs, (2) the combined active area remains constant, i.e., the active areas of the individual PDs shrink. We provide intuition to guide the design of next-generation PD array-based systems. The contributions of this letter are as follows.

- We develop a model for the signal-to-noise ratio (SNR) and achievable rates for PD array-based receivers, taking into account the square-law relationship between the optical and electrical powers as well as the impact of the PD size on bandwidth.
- We introduce a *loss factor* and use it to model the extent of suboptimality for different beam patterns, and to compare the performance of PD array-based receivers for the two considered design choices with that of a reference receiver employing a single PD.

Through analysis and numerical simulations, we show that PD arrays provide a performance gain when the incident beam is sufficiently narrow and when the received SNR is above a threshold, which depends on the incident beam pattern. Furthermore, we show that, in most cases, the performance of the reference receiver can be exceeded by increasing the received power and not by increasing the number of PDs alone. Lastly, we show that, for PD array-based receivers, direct detection of higher-order transverse electromagnetic laser beam modes is suboptimal, and a mode conversion to the fundamental Gaussian beam is beneficial.

The remainder of this paper is organized as follows. In Section II, we introduce the receiver model and review the factors affecting the bandwidth of PDs. Furthermore, we describe the considered beam patterns. In Section III, we derive the performance scaling laws. Numerical results and discussions are provided in Section IV, and the paper is concluded in Section V.

II. PRELIMINARIES

In this section, we provide the receiver model, discuss briefly the factors affecting PD bandwidth, and describe the

considered laser beam patterns.

A. Receiver Model

We consider a point-to-point IM/DD OWC system comprising a transmitter and a receiver, and focus on the receiver design. The receiver is composed of a PD array with M identical PDs and employs linear signal processing to combine the received signals from the PDs, after the TIA, in the electrical domain. Let the *optical* power received by the m-th PD be denoted by $P_m^{\mathrm{Rx,O}}$, $m=1,...,M$, and let $P_{\mathrm{tot}}^{\mathrm{Rx,O}} = \sum_{m=1}^{M} P_m^{\mathrm{Rx,O}}$ denote the total received power. The received *electrical* power for the m-th PD is given by $P_m^{\mathrm{Rx,E}} = (R_{\mathrm{PD}} P_m^{\mathrm{Rx,O}})^2$ as an inherent consequence of square-law detection [15], [18], where R_{PD} denotes the responsivity of the PDs in A/W, which is assumed to be identical for all PDs. Furthermore, let B and N_0 denote the bandwidth and the thermal noise power spectral density of a PD, respectively, which are also assumed to be identical for all PDs[1]. Moreover, we consider OWC in the thermal noise limited regime where the impact of shot noise and relative intensity noise is considered negligible [12]. Hence, the SNR for the m-th PD, $m=1,...,M$, is given by

$$\gamma_m = \frac{(R_{\mathrm{PD}} P_m^{\mathrm{Rx,O}})^2}{B N_0}. \tag{1}$$

Next, we describe the area-bandwidth trade-off of PDs.

B. Area-Bandwidth Trade-Off

The 3-dB bandwidth of a PD is given by $B = \frac{1}{\sqrt{(2\pi R_{\mathrm{L}} C_{\mathrm{j}})^2 + (2\pi t_\tau)^2}}$ [14], where $C_{\mathrm{j}} = \frac{\epsilon A}{d}$ denotes the junction capacitance and ϵ, A, and d denote the junction permittivity, area, and thickness, respectively, R_{L} denotes the load resistance, and t_τ denotes the junction carrier transit time. As has been shown in [14], when the bandwidth is limited by the junction capacitance, $B \propto \frac{1}{A}$ holds, while when it is limited by the carrier transit time, B is independent of A, and when the junction thickness is optimized for the maximum bandwidth, then $B \propto \frac{1}{\sqrt{A}}$, see also [12]. We consider all three regimes. Furthermore, in order to identify the most beneficial operating regime of the PD array, we compare its performance with that of a single reference PD of fixed bandwidth B_0 and the same total active area. This ensures that the effect of bandwidth expansion due to the changed active area of the PDs when scaling the PD array is properly taken into account. Moreover, we assume that, in all three cases above, the initial bandwidth of the PD array, i.e., for $M=1$, is B_0.

Next, we define optical power distribution patterns, which will be considered throughout the letter.

C. Considered Laser Beam Patterns

In the following, we consider four laser beam patterns. The degenerate and uniform beam patterns serve as edge cases for the laser beam power distribution. On the other hand, Gaussian and LG$_{10}$ beam patterns, which we consider as representative patterns for our study, are the more practical schemes.
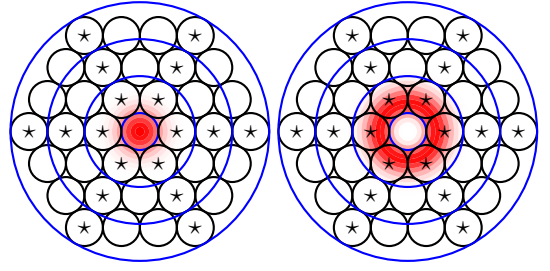

Fig. 1. Illustration of the beam power distribution for Gaussian and LG$_{10}$ beams with $G=3$ rings and $\rho=0.5$ on a PD array employing the optimal hexagonal packing. PDs marked with a $\star$ denote the six corner PDs in each ring.

For the degenerate beam pattern, we have $P_1^{\mathrm{Rx,O}} = P_{\mathrm{tot}}^{\mathrm{Rx,O}}$ and $P_m^{\mathrm{Rx,O}} = 0$, $m=2,...,M$, up to permutation. That is, the PD with index 1 receives all the power and the other PDs do not receive any optical signal.

Next, for the uniform optical received power distribution, we have $P_m^{\mathrm{Rx,O}} = \frac{P_{\mathrm{tot}}^{\mathrm{Rx,O}}}{M}$, for $m=1,...,M$. That is, all the PDs receive the same optical power.

Next, we consider the Gaussian[2] and LG$_{10}$ beam patterns. We note that the Gaussian beam concentrates energy close to the center, whereas the LG$_{10}$ beam has the energy concentrated in a ring around a central vortex, as shown in Figure 1.

Furthermore, for these beams, since the captured energy depends on the placement of the PDs in the PD array, we assume the optimal hexagonal packing[3], which covers about 90% of the circular area [19]. Furthermore, we assume that M has the form $M = 1 + 3G(G+1)$, for some non-negative integer G. This enables positioning a central PD aligned to the incident beam center, and G concentric hexagonal rings in the periphery, where the g-th ring contains $6g$ PDs. The pattern is illustrated in Figure 1 for the Gaussian and LG$_{10}$ modes for $G=3$ and $\rho=0.5$. Throughout this letter, ρ denotes the ratio of the PD radius to the beam waist.

Next, based on [19], [20], for the Gaussian beam, the received optical power for the central PD is given by

$$P_1^{\mathrm{Rx,O}} = \frac{(1-\mathrm{e}^{-2\rho^2})}{1-\mathrm{e}^{-2(G+1)^2\rho^2}} P_{\mathrm{tot}}^{\mathrm{Rx,O}}, \tag{2}$$

where the expressions in the numerator and denominator are obtained by Gaussian radial integration and are the received optical powers for the central and reference PDs, respectively, and their ratio denotes the fraction of the total power received by the central PD. Furthermore, the received optical power for the six corner PDs on ring g, $g=1,...,G$, which are marked with a $\star$ in Figure 1, is given by

$$P_{\mathrm{Gauss,c},g}^{\mathrm{Rx,O}} = \frac{(1-Q_1(4g\rho, 2\rho))}{1-\mathrm{e}^{-2(G+1)^2\rho^2}} P_{\mathrm{tot}}^{\mathrm{Rx,O}}, \tag{3}$$

---

[1]As noted later, the developed results and intuitions are also valid for unequal responsivities and noise power spectral densities.

[2]We note that the fundamental LG$_{00}$ mode is equivalent to the Gaussian beam.

[3]We note that, although in this letter we limit ourselves to representative LG modes and the optimal hexagonal packing, the methods described can be extended to arbitrary modes and positions of PDs within the PD array in a straightforward manner.

and for the remaining $(6g-6)$ PDs, which are unmarked in Figure 1, it is given by

$$P_{\text{Gauss},e,g}^{\text{Rx,O}} = \frac{(1-Q_1(2\sqrt{3}g\rho,2\rho))}{1-e^{-2(G+1)^2\rho^2}}P_{\text{tot}}^{\text{Rx,O}}. \tag{4}$$

Here, $Q_m(a,b)$ denotes the Marcum's Q function of order m. Analogously, based on [21], [22], for the LG$_{10}$ beam, the received optical power for the central PD is given by

$$P_1^{\text{Rx,O}} = \frac{(1-e^{-2\rho^2}-2\rho^2e^{-2\rho^2})P_{\text{tot}}^{\text{Rx,O}}}{1-e^{-2(G+1)^2\rho^2}-2(G+1)^2\rho^2e^{-2(G+1)^2\rho^2}}. \tag{5}$$

Furthermore, the received optical power for the six corner PDs on ring g, $g=1,...,G$, is given by

$$P_{\text{LG}_{10},c,g}^{\text{Rx,O}} = \frac{\phi(2g\rho,\rho)P_{\text{tot}}^{\text{Rx,O}}}{1-e^{-2(G+1)^2\rho^2}-2(G+1)^2\rho^2e^{-2(G+1)^2\rho^2}}, \tag{6}$$

and, for the remaining $(6g-6)$ PDs, it is given by

$$P_{\text{LG}_{10},e,g}^{\text{Rx,O}} = \frac{\phi(\sqrt{3}g\rho,\rho)P_{\text{tot}}^{\text{Rx,O}}}{1-e^{-2(G+1)^2\rho^2}-2(G+1)^2\rho^2e^{-2(G+1)^2\rho^2}}, \tag{7}$$

where $\phi(a,b) = 2a^2(1-Q_2(2a,2b)) + (1-Q_1(2a,2b)) - 2b^2e^{-2(a^2+b^2)}I_0(4ab)$, and $I_0(x)$ is the modified Bessel function of the first kind and order zero.

Next, we derive the performance scaling laws.

III. COMBINING IN THE ELECTRICAL DOMAIN

In this section, we analyze the impact of combining in the electrical domain and derive the performance scaling laws for IM/DD systems employing PD arrays.

A. Optimal SNR

First, we note that for maximal ratio combining, which is the optimal linear combining scheme, the SNR, γ_{mrc}, is given by $\gamma_{\text{mrc}} = \sum_{m=1}^{M}\gamma_m$, whose maximum value depends on the input optical power distribution, which can be optimized as

$$\{P_m^{\text{Rx,O}\star},\forall m\} = \underset{\substack{\{P_m^{\text{Rx,O}},\forall m\} \\ \sum_{m=1}^{M}P_m^{\text{Rx,O}}\leq P_{\text{tot}}^{\text{Rx,O}}}}{\arg\max} \gamma_{\text{mrc}}. \tag{8}$$

Based on [23, Theorem C.1 and Equation (8)], Problem (8) is Schur-convex, and the optimal received optical power distribution is degenerate[4], up to permutation, see Section II-C. Hence, for optimal performance, the received beam must be incident on a single PD in the PD array in order to minimize the loss due to the square-law relationship between the optical and electrical powers. In such a case, the optimal SNR is given by $\gamma_{\text{mrc}}^{\star} = \frac{(R_{\text{PD}}P_{\text{tot}}^{\text{Rx,O}})^2}{BN_0}$. Hence, beam patterns such as Gaussian, vortex beams, uniform beams, and other higher-order transverse electromagnetic beams do not achieve the maximum SNR in general. Nevertheless, focusing all power on a single PD of the PD array is impractical due to alignment considerations and the law of étendue conservation, which disallows arbitrary concentration of beams. Next, in the following, we model the extent of *suboptimality* of the considered practical beams.

B. Loss Factor

In order to derive insights for the practical case, where the received optical power distribution is not degenerate, we define the actually achieved (suboptimal) SNR as

$$\gamma_{\text{sub}} = \frac{(\beta R_{\text{PD}}P_{\text{tot}}^{\text{Rx,O}})^2}{BN_0} = \beta^2\gamma_{\text{mrc}}^{\star}, \tag{9}$$

where β, $0\leq\beta\leq1$, is the *loss factor*, which models the suboptimality of the PD design and incident beam with a single parameter. In the following, we utilize the above model based on γ_{sub} for analyzing arbitrary beam power distributions, including Gaussian, LG$_{10}$, and uniform beams, incident on the hexagonal PD arrangement described earlier.

C. Performance Comparison with the Reference PD

From Section II-B, we note that the bandwidth B of the PDs scales as $B = M^\xi B_0$, where $\xi = 1,\frac{1}{2}$, and 0 for capacitance limited, thickness optimized, and transit-time limited PDs, where the active area of the individual PDs is assumed to be $\frac{1}{M}$-th of the reference PD. Hence, the achievable rate, R, for the PD array is given by the Shannon formula[5] as

$$R = M^\xi B_0\log\left(1+\beta^2\frac{\gamma_{\text{mrc}}^{\star}}{M^\xi}\right). \tag{10}$$

For a PD array with $M>1$ PDs to have a better performance than the single reference PD,

$$R\geq B_0\log(1+\gamma_{\text{mrc}}^{\star}) \tag{11}$$

must be satisfied, which leads to the condition

$$\beta^2\geq\beta_{\min}^2 = \frac{M^\xi}{\gamma_{\text{mrc}}^{\star}}\left[(1+\gamma_{\text{mrc}}^{\star})^{\frac{1}{M^\xi}}-1\right]. \tag{12}$$

Hence, for $\beta^2\geq\beta_{\min}^2$, which is discussed in detail below, a PD array meets or exceeds the performance of the single reference PD. Therefore, ideally, $\beta_{\min}^2$ must be as low as possible to establish a low barrier. On the other hand, when $\beta^2<\beta_{\min}^2$, PD arrays offer no performance benefit over the single reference PD, but may have other advantages such as misalignment tolerance and fabrication ease, see, e.g., [9], [11], among others.

1) Impact of Scaling $\gamma_{\text{mrc}}^{\star}$: We note that $\lim_{\gamma_{\text{mrc}}^{\star}\to\infty}\beta_{\min}^2 = 0$ for all ξ. Hence, $\beta_{\min}^2$ can be made arbitrarily small by increasing the received SNR, $\gamma_{\text{mrc}}^{\star}$, sufficiently. This enables us to meet or exceed the reference PD performance for arbitrary β^2, see Section III-D3.

2) Impact of Scaling M: Next, we note that for $\xi = 1,\frac{1}{2}$, $\lim_{M\to\infty}\beta_{\min}^2 = \frac{\log(1+\gamma_{\text{mrc}}^{\star})}{\gamma_{\text{mrc}}^{\star}}$, indicating that for both capacitance and thickness optimized devices, $\beta_{\min}^2$ has an asymptotic floor. Hence, unlike with SNR, $\beta_{\min}^2$ cannot be made arbitrarily small. Therefore, scaling M alone is not sufficient to meet the reference PD performance. On the other hand, for $\xi = 0$, $\lim_{M\to\infty}\beta_{\min}^2 = 1$, indicating that only the degenerate received optical power distribution meets the reference PD performance.

---

[4]We note that, based on [23, Theorem C.1 and Equation (8)], the degenerate distribution is optimal also when the responsivity and noise variance of the PDs are not identical.

[5]We note that although we utilize the Shannon formula to analyze the impact of bandwidth on performance, the insights obtained in this paper are also applicable to the upper and lower bounds in [2], [3].

D. Loss Factor for the Considered Distributions

For the degenerate distribution, $\beta^2_{\text{degen}} = 1$, and for the uniform optical received power distribution, $\beta^2_{\text{unif}} = \frac{1}{M}$. On the other hand, for a Gaussian beam, β^2 can be simplified to

$$\beta^2_{\text{Gauss}} = \frac{(1-e^{-2\rho^2})^2 + \sum_{g=1}^{G} 6(1-Q_1(4g\rho, 2\rho))^2}{(1-e^{-2(G+1)^2\rho^2})^2}$$
$$+ \frac{\sum_{g=1}^{G}(6g-6)(1-Q_1(2\sqrt{3}g\rho, 2\rho))^2}{(1-e^{-2(G+1)^2\rho^2})^2}, \quad (13)$$

and for the LG_{10} beam to

$$\beta^2_{\text{LG}_{10}} = \frac{(1-e^{-2\rho^2}-2\rho^2 e^{-2\rho^2})^2 + \sum_{g=1}^{G} 6\phi(2g\rho, \rho)^2}{(1-e^{-2(G+1)^2\rho^2}-2(G+1)^2\rho^2 e^{-2(G+1)^2\rho^2})^2}$$
$$+ \frac{\sum_{g=1}^{G}(6g-6)\phi(\sqrt{3}g\rho, \rho)^2}{(1-e^{-2(G+1)^2\rho^2}-2(G+1)^2\rho^2 e^{-2(G+1)^2\rho^2})^2}. \quad (14)$$

We note that as $\rho \to 0$ and $G \to \infty$, β^2_{Gauss} and $\beta^2_{\text{LG}_{10}}$ approach G^{-1} and G^{-3}, respectively. On the other hand, for $\rho > 1$, the whole beam waist falls within the central PD, resembling the degenerate beam, see also Figure 1. Hence, $\rho \to 0$ represents the practically relevant case.

1) Central PD Only: For the case where only the central PD is utilized, whose bandwidth, unlike the reference PD, scales with the active area, then, as $\rho \to 0$, $\beta^2_{\text{Gauss},1}$ and $\beta^2_{\text{LG}_{10},1}$ approach G^{-2} and G^{-4}, respectively. Hence, they are asymptotically inferior compared to utilizing the entire PD array[6].

2) Higher-Order LG Modes: We note that $\frac{\beta^2_{\text{Gauss}}}{\beta^2_{\text{LG}_{10}}} \sim G^2$ as $\rho \to 0, G \to \infty$, which shows that the Gaussian beam is asymptotically superior compared to the LG_{10} beam owing to the vortex of the latter and the greater spreading of the incident power, see also Section IV. The same insight applies to other higher order modes, which spread their incident power over larger areas compared to the Gaussian beam.

3) Received Power Scaling: For a design with loss factor β^2, the performance of the reference PD can be met by increasing the received *optical* power by $\alpha = \sqrt{\frac{\beta^2_{\text{min}}}{\beta^2}}$. We note that for the practically relevant case of $\rho \to 0$, we have $\lim_{\rho \to 0}\lim_{G \to \infty}\alpha_{\text{Gauss}} = \infty$ and $\lim_{\rho \to 0}\lim_{M \to \infty}\alpha_{\text{LG}_{10}} = \infty$, i.e., for suboptimal systems with $\beta^2 < \beta^2_{\text{min}}$, the received power must continually increase with increasing G in order to meet the reference PD performance.

IV. NUMERICAL RESULTS AND DISCUSSION

In this section, we present numerical results, along with a discussion.

First, we study the minimum loss factor β^2_{min}, which incorporates the effects of bandwidth expansion and SNR via ξ and $\gamma^\star_{\text{mrc}}$, respectively, as a function of the number of PDs M. Figure 2 illustrates β^2_{min} as a function of M for different SNR and ξ values, based on (12). The figure shows that, for $\xi = 1, \frac{1}{2}$, β^2_{min} converges rapidly to the respective asymptotic value given in Section III-C, indicating that increasing M alone yields no improvement over the single reference PD performance. Furthermore, for small M, thickness-optimized

[6]We note that the "Central PD Only" case is impractical for LG_{10} since the central PD always lies in the vortex.
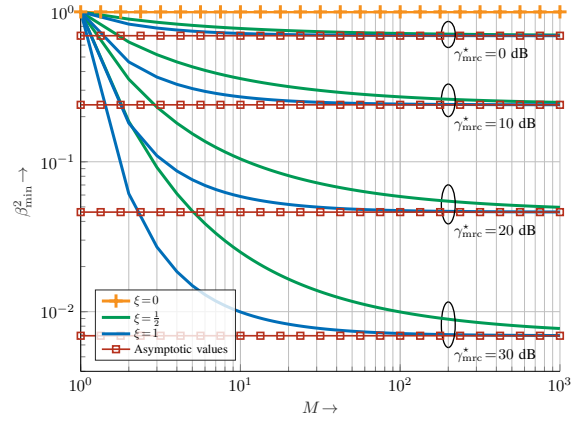

Fig. 2. Minimum required loss factor β^2_{min} as a function of M for different SNRs, based on (12).
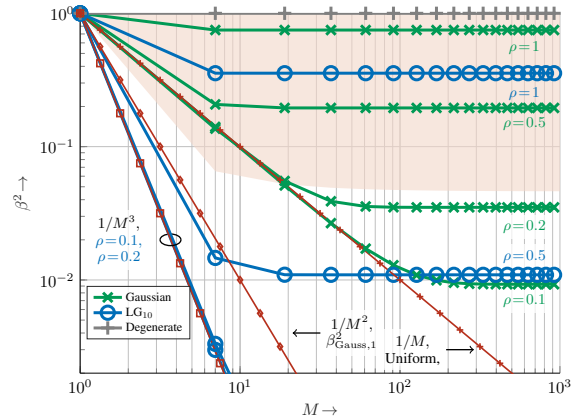

Fig. 3. Loss factor β^2 versus the number of photodetectors M for Gaussian and LG_{10} beams with fixed PD-radius-to-beam-waist ratio ρ.

PDs are slightly inferior compared to capacitance limited ones. Nevertheless, they perform similarly asymptotically. Moreover, as the SNR increases, the required β^2_{min} decreases significantly. This validates the analytical observation that PD arrays become beneficial above a certain SNR threshold, where the bandwidth gain achieved by reducing the PD area outweighs the electrical power loss caused by the square-law relationship, see Section III. On the other hand, for $\xi = 0$, β^2_{min} is independent of M.

Next, in the following figures, we study the the loss factor β^2, which models the effects of beam shape and parameters, array PD positions, and the impact of square-law. Figure 3 shows β^2 versus M for Gaussian and LG_{10} beams[7] when the PD-radius-to-beam-waist ratio ρ is kept constant, along with the asymptotic values discussed in Section III. In this case, with increasing M, the overall active area of the PD array increases. The results show that for small ρ, both modes exhibit a rapid decay of β^2, with LG_{10} degrading substantially faster than Gaussian owing to its vortex and greater power spread. Comparatively, the uniform beam experiences an intermediate performance degradation. For larger ρ, where most of the optical power is concentrated on the central PD, β^2 approaches unity, which is consistent with the degenerate distribution. These results highlight the strong dependence of performance on beam concentration and
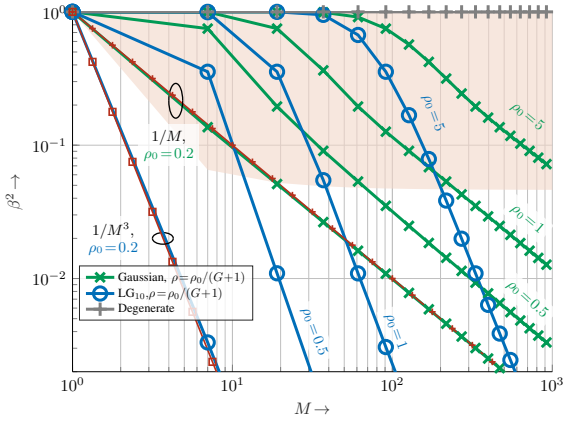
[7]Only values of $M = 1 + 3G(G+1)$ are reported.

Fig. 4. Loss factor β^2 versus the number of photodetectors M when the PD radius scales inversely with array size, $\rho = \rho_0/(G+1)$.

validate the suboptimality of direct detection of higher-order modes. Lastly, in this and the next figures, pink shading denotes the region in which $\beta^2 \geq \beta^2_{\min}$ for $\xi = 1$ and $\gamma^\star_{mrc} = 20$ dB.

Next, Figure 4 considers a more practical scenario, where ρ decreases with increasing array size as $\rho = \rho_0/(G+1)$. This corresponds to the case where the PD radius shrinks with M, while the reference PD size remains constant. Here, the effective beam footprint becomes increasingly spread over the PD array as M grows. Hence, β^2 degrades for increasing M for both modes, and the gap between Gaussian and LG_{10} widens. This result shows that, for realistic receiver scaling, increasing the number of PDs exacerbates the square-law penalty unless the received beam remains sufficiently narrow.

Nevertheless, in both cases, the performance of the reference PD is exceeded whenever $\beta^2 > \beta^2_{\min}$ for the designed system parameters. Furthermore, the results are consistent with the analysis in Section III. Gaussian beams behave like uniform beams for small ρ and like degenerate beams for large ρ, whereas higher-order LG modes have a substantially larger penalty due to their spatially distributed intensity profiles. Therefore, for PD array-based IM/DD receivers, meeting or exceeding the performance of a single reference PD generally requires careful parameter choice or increasing the received power rather than merely scaling the number of PDs. Furthermore, based on the large performance penalty, we note that converting higher-order spatial modes to the fundamental Gaussian mode prior to direct detection is advantageous in practice. The above results highlight the need for joint optimization of beam pattern, transverse electromagnetic mode, received power, and PD positions.

V. Conclusion

We studied performance scaling laws for PD array-based receivers in IM/DD optical wireless systems by explicitly accounting for the inherent square-law relationship between optical and electrical powers. By comparing PD arrays to a reference single-PD receiver for Gaussian, LG_{10}, and uniform beam patterns and for different PD area scaling assumptions, we showed that PD arrays provide performance gains for sufficiently narrow beams and above an SNR threshold, depending on the loss factor β^2. Furthermore, increasing M alone does not exceed reference PD performance, and, in most cases, received optical power

must be scaled by $\sqrt{\frac{\beta^2_{\min}}{\beta^2}}$ to meet it. Moreover, direct detection of higher-order modes, which spread power over several PDs, is generally suboptimal, and conversion to the fundamental Gaussian beam before detection is beneficial. These results provide clear guidelines and highlight the trade-offs in designing next-generation high-bandwidth PD array receivers.

References

[1] N. Gupta and M. S. Alouini, "Coherent optical wireless systems: Progress and challenges," *IEEE Commun. Surveys Tuts.*, vol. 21, pp. 2998–3024, 2019.

[2] A. Lapidoth, S. M. Moser, and M. A. Wigger, "On the capacity of free-space optical intensity channels," *IEEE Trans. Inf. Theory*, vol. 55, pp. 4449–4461, 2009.

[3] A. Chaaban and S. Hranilovic, "Capacity of optical wireless communication channels," *Philosophical Transactions of the Royal Society A: Mathematical, Physical and Engineering Sciences*, vol. 378, p. 20190184, 2020.

[4] M. A. Fernandes, P. P. Monteiro, and F. P. Guiomar, "Free-space terabit optical interconnects," *Journal of Lightwave Technology*, vol. 40, pp. 1519–1526, 2022.

[5] C. St-Arnault, S. Bernal, D. Kita *et al.*, "Net 3.2 Tbps 225 Gbaud PAM4 O-Band IM/DD 2 km transmission using FR8 and DR8 with a CMOS 3 nm SerDes and TFLN modulators," in *Proc. Optical Fiber Commun. Conf. and Exhib. (OFC)*, 2025, pp. 1–3.

[6] A. Chaaban, J. M. Morvan, and M.-S. Alouini, "Free-space optical communications: Capacity bounds, approximations, and a new sphere-packing perspective," *IEEE Trans. Commun.*, vol. 64, pp. 1176–1191, 2016.

[7] H. Haas, L. Yin, Y. Wang, and C. Chen, "What is LiFi?" *J. Lightwave Technol.*, vol. 34, pp. 1533–1544, 2019.

[8] Z. Zeng, J. Li, and Z. Wu, "Imaging receivers for visible light communication: Principles and advances," *Optics Express*, vol. 25, pp. 27 011–27 026, 2017.

[9] T. Koonen, K. Mekonnen, F. Huijskens *et al.*, "Novel broadband OWC receiver with large aperture and wide field-of-view," in *European Conference on Optical Communications (ECOC)*, Dec. 2020.

[10] M. Madhavan and C. Gong, "Large-area photodiode array architectures for high-sensitivity optical receivers," *IEEE Photonics Technol. Lett.*, vol. 32, pp. 825–828, 2020.

[11] T. Umezawa, Y. Yoshida, A. Kanno *et al.*, "FSO receiver with high optical alignment robustness using high-speed 2D-PDA and space diversity technique," *Journal of Lightwave Technology*, vol. 39, pp. 1040–1047, 2021.

[12] E. Sarbazi, H. Kazemi, M. Crisp *et al.*, "Design and optimization of high-speed receivers for 6G optical wireless networks," *IEEE Trans. Commun.*, vol. 72, pp. 971–990, 2024.

[13] Z. Jiang, X. Su, H. Zhou *et al.*, "Demonstration of photodetector-array-based reconfigurable mode division-multiplexing coherent receiver for spatial modes varying two indices," in *Proc. Europ. Conf. Optical Commun. (ECOC)*, 2025.

[14] S. B. Alexander, *Optical Communication Receiver Design*, ser. IEE Telecommunications Series. Bellingham, Wash., USA: SPIE, 1997.

[15] J. M. Kahn and J. R. Barry, "Wireless infrared communications," *Proc. IEEE*, vol. 85, pp. 265–298, 1997.

[16] G. P. Agrawal, *Fiber-Optic Communication Systems*. John Wiley & Sons, Ltd, 2010.

[17] M. S. Bashir, "Free-space optical communications with detector arrays: A mathematical analysis," *IEEE Trans. Aerosp. Electron. Syst.*, vol. 56, pp. 1420–1429, 2020.

[18] S. Hranilovic, *Wireless Optical Communication Systems*. Springer New York, 2005.

[19] L. Fukshansky, "Revisiting the hexagonal lattice: On optimal lattice circle packing," *Elemente der Mathematik*, vol. 66, pp. 1–9, Jan. 2011.

[20] C. Azzolin, A. F. Gurgel, and V. G. A. Carneiro, "Marcum Q-function as an analytical solution for misaligned Gaussian beams," *Optical Engineering*, vol. 60, p. 056105, 2021.

[21] A. A. Kovalev, V. V. Kotlyar, and A. P. Porfirev, "Asymmetric Laguerre-Gaussian beams," *Physical Review A*, vol. 93, p. 063858, Jun. 2016.

[22] M. Simon, "The Nuttall Q function - its relation to the Marcum Q function and its application in digital communication performance evaluation," *IEEE Trans. Commun.*, vol. 50, pp. 1712–1715, Nov. 2002.

[23] A. W. Marshall, I. Olkin, and B. C. Arnold, *Inequalities: Theory of Majorization and Its Applications*. Springer New York, 2011.